INSTITUTO DE INGENIERÍA ENERGÉTICA
UNIVERSIDAD POLITÉCNICA DE VALENCIA

CPI, Edificio 8E, Cubo F, 5ª planta, Camino de Vera s/n, 46022 Valencia, Spain Tel. (34) 963877270, Fax (34) 963877272, Email: energeti@upvnet.upv.es

INSTITUTO DE INGENIERÍA ENERGÉTICA
(Institute for Energy Engineering)

Research Publications

Optimized design of a heat exchanger for an air-to-water reversible heat pump working with propane (R290) as refrigerant: Modelling analysis and experimental observations

J. Blanco Castro *, J.F. Urchueguía, J.M. Corberán, J. Gonzálvez

Investigación y Modelado de Sistemas Térmicos, Universidad Politécnica de Valencia, Camino de Vera, 14, 46022 Valencia, Spain

Received 15 September 2004; accepted 10 December 2004
Available online 23 February 2005

Abstract

An experimental study of an air-to-water reversible heat pump unit was carried out using two different fin-and-tube heat exchanger "coil" designs and propane (R290) as the working fluid. The main aim of these tests was to search for optimized coil design concepts. The performance of the heat pump was evaluated for each coil design at different superheat conditions at the inlet of the compressor in both modes of operation: heating and cooling. Coefficient of Performance (COP) in both modes of each heat pump unit using two different coil design are presented. Experimental measurements are compared against model predictions. The mean refrigerant side heat transfer coefficient and the pressure drop as a function of mass flux along the flow path are calculated. As a results of tests, it was found that the performance was obtained in the heat pump unit using coil-2 design with less refrigerant circuit and a higher length of circuit with a superheat of around 6 K in both modes of operation. From the calculation it was found that in both modes of operation coil-2 design gives higher heat transfer coefficients and pressure drops for the refrigerant side.

* Corresponding author. Tel.: +34 96 387 9323; fax: +34 96 387 3329.
E-mail address: jblancoc@ter.upv.es (J. Blanco Castro).
URL: http://www.imst.upv.es (J. Blanco Castro).

1359-4311/$ - see front matter
doi:10.1016/j.applthermaleng.2004.12.009

Keywords: Heat pump; Propane; Coefficient of Performance; Heat exchangers

1. Introduction

Due to ozone depletion that leads to global warming effects, environmental friendly refrigerants with null ozone depletion (ODP) and low global warming potential (GWP) are required for the new generation of refrigerators and air conditioners. Hydrocarbon refrigerants such as propane (R290)—with nearly zero ODP— have been recommended by several authors, [1–7], to be used as working fluid in air conditioning and heat pump systems. Some of these studies confirmed that propane may offer significant increases in performance. This is specially true if the plant is conceived to take advantage of its specific thermo-physical characteristics in comparison with R22.

During the last years, a lot of work was done to analyze the influence of heat transfer characteristics in fin-and-tube heat exchangers on performance. Nan and Ferreira [8] investigated the heat transfer coefficients in evaporation and condensation in smooth, micro fin and crosshatched outside diameter copper tubes of 9.52 mm using R290 as refrigerant. The authors compared the experimental data with different correlations for smooth tubes, and their results confirmed that the Shah [9] and Cavallini–Zecchin [10] correlations provide the most reliable heat transfer coefficients.

Rice [11] investigated the relationship between the number of circuits and the inner tube diameter on the performance of an air-to-air reversible heat pump working with R22 and the alternative work fluids, such as R134a, R410A and R290. He found that with R410A and R290, the optimal tubes are one tube size smaller than for R22 with the similar numbers of circuits. In addition, R290 requires one extra circuit with respect to R410A for both heat exchangers (indoor and outdoor coils). The reduction in tube sizes for R410A and R290 results in 20–67% lower charge requirements than for R22. Concerning the outdoor coils with tube ID of 7.9 mm coupled with R410A and R290, they deliver slightly lower performance with significantly lower charge while requiring one additional circuit.

On the other hand, Liang et al. [12] analyzed the performances of evaporator coils with several ''complex'' refrigerant circuitry using a distributed simulation model, and obtained the heat transfer characteristics of R134a evaporation in four different circuit configurations. Their results demonstrate that the coil performance can be improved by changing the mass flux along the each path defining the configuration. Distributing the refrigerant mass flux along different paths of the heat exchanger should be a reasonable approach to balance the increments in the refrigerant heat transfer and pressure drop. Bigot et al. [13] measured the performance of a coil with 7 mm outside tube diameter using R407C in a reversible heat pump. The outcome of the test showed that an appropriate design of the air-refrigerant counter flow heat exchanger using R407C allows a 20% increase in the global heat exchange coefficient at the evaporator and 10% at the condenser.

The central objective of our work is to analyze the influence of different coil designs on the behavior of an air-to-water reversible heat pump using R290 as refrigerant. The performance of a heat pump system is measured for two different fin-and-tube heat exchanger (coil) designs at several superheat conditions at the compressor inlet in both modes: heating and cooling. The heat transfer coefficient (HTC) and pressure drops for the refrigerant side as a function of mass flux are studied

Nomenclature

COP	Coefficient of Performance
c_p	specific heat capacity ($kJ\,kg^{-1}\,K^{-1}$)
d_i	inner tube diameter (m^2)
$G^{\bullet}$	refrigerant mass flux ($kg\,m^{-2}\,s^{-1}$)
HTC	heat transfer coefficient ($W\,m^{-2}\,K^{-1}$)
HEX	heat exchanger
$m^{\bullet}$	mass flow rate ($kg\,s^{-1}$)
N_c	number of circuits
$Q^{\bullet}$	heat exchanger capacity (kW)
T	temperature (K)

Subscripts

i	internal
in	inlet
out	outlet
r	refrigerant
wat	water

for both modes of operation and coil designs using a model capable of simulating the heat pump, see Corberán et al. [14]. A by-product of this investigation elucidates the identification of a new coil design to improve the efficiency of an air-to-water reversible heat pump using R290 as working fluid.

2. Experimental setup and test procedure

The heat pump test rig shown in Fig. 1 was designed to perform the characterization of a medium size, reversible air-to-water heat pump. The test rig components are: a climatic chamber, air treatment unit, hydraulic group and the heat pump unit.

2.1. Climatic chamber

The entire range of climate conditions typical of Southern Europe can be adequately simulated in a 50 m^3 climatic chamber in both modes, heating and cooling. The air-side-coil of the heat pump unit is attached to the climatic chamber ensuring, by means of a variable fan, that the air pressure drop across the unit is null. An air treatment unit is located on the top of the climatic chamber and creates the desired environmental conditions inside the chamber by adequately mixing outdoor air and the return air from the heat pump. The temperature regulation in the climatic chamber was done by means of a control unit, which while using the air temperature measurements in the duct and outdoors, controlled the outdoor damper and the recirculating damper. Temperature measurements were accurately done using humidity and temperature transmitters.

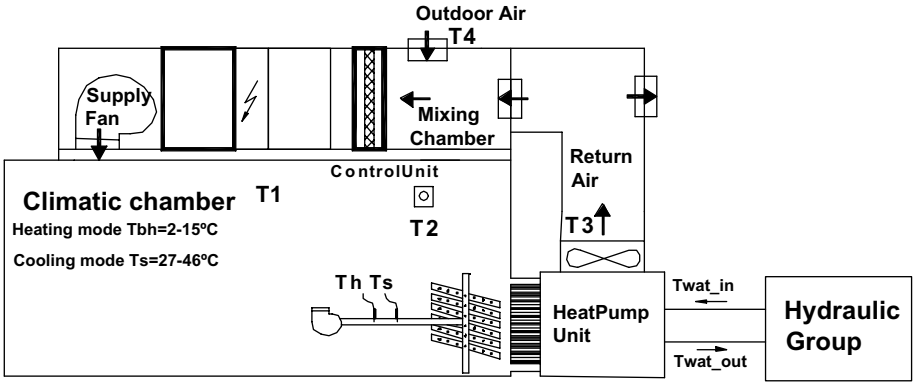

Fig. 1. Schematic of the heat pump test rig.

The air temperature regulation in the climatic chamber allowed the attainment of a maximum temperature of 46 °C and a minimum temperature of 2 °C.

2.2. Hydraulic loop

In the water-side of the heat pump unit, an hydraulic loop simulates the loads of the unit, ensuring that the standard operating conditions are maintained in the refrigerant-to-water brazed plate heat exchanger (BPHE). The hydraulic group consists of a deposit of inertia, an expansion vessel, to muffle possible fluctuations due to changes in the water temperature or pressure, a brazed plate heat exchanger, a three ways motorized valve, a manual valve and a sensor to measure the flow of water.

The regulation system consists of a controller universal type PID, which receives the signal from an immersion temperature sensor, type PT-100, placed at the entrance of the water in the heat pump, which acts on the motorized three ways valve. This allows to regulate the flow of water through the BPHE and the temperature to the exit of the BPHE. Acting on the manual valve, the flow of water entering in the heat pump is regulated fixing thus the required temperature difference in agreement with the operation conditions. Temperature difference, which is critical for a precise measurement, was determined by means of a pair of carefully calibrated PT-100-type thermo-resistance probes. In all the test during the characterization of the different designs, the thermal jump was regulated to get a difference of temperature among the outlet/inlet of the BPHE of ± 5 K.

2.3. Heat pump instrumentation and safety

The heat pump unit was placed outside of the climatic chamber. The heat pump used for the test is a modified version of an R22 catalogue model of CIATESA (IWA-95), specifically adapted, from the point of view of safety as well as performance, to be used with propane as refrigerant. All materials and measurement devices utilized were intrinsically safe. Gas detectors were also installed in the reference heat pump in combination with a switch isolating the electrical circuits according to the Spanish norm UNE 20-318 for electrical components in atmospheres with

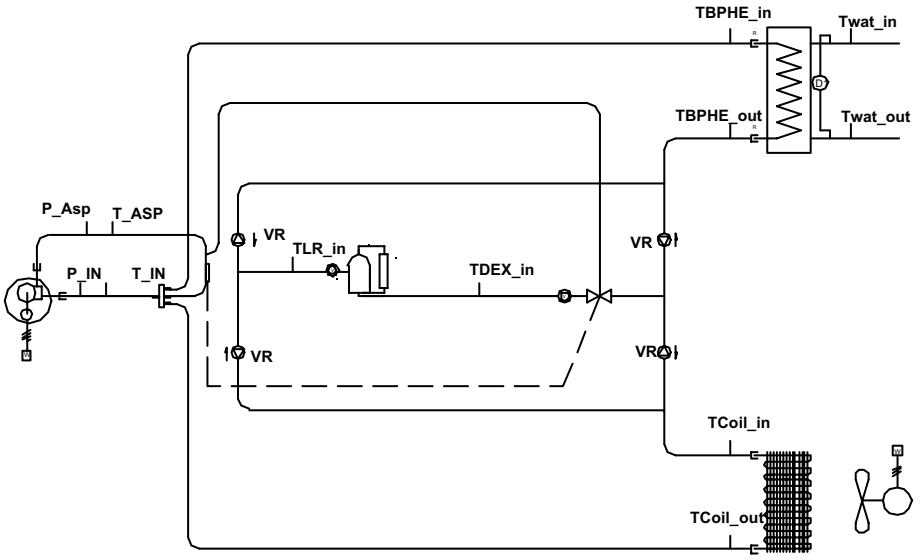

Fig. 2. Instrumented heat pump test rig.

potential flammable vapours or gases and the UNE-EN 60079-10 for electrical materials in explosive atmospheres.

The heat pump unit (Fig. 2) is equipped with a scroll compressor, a thermostatic expansion valve, a BPHE with 46 plates and a fin-and-tube heat exchanger that acts as condenser/evaporator. It is thoroughly instrumented with several resistance temperature detectors, absolute pressure transducers and relative pressure meters. Inside the heat pump, the evaporation and condensation pressure were determined by means of pressure sensors located up-and-down stream of the compressor. A digital energy counter was used to measure compressor power consumption. Several PT-100 thermo-resistance temperature probes were placed to measure the levels of superheat and subcooling. A data acquisition system collected the information related to temperatures, pressures, secondary loop water mass flow rates, air humidity and compressor power input measurements. The specification along with the uncertainties of the sensors are summarized in Table 1.

Table 1
Characteristics of instrumentation employed in the heat pump test rig

Parameter	Uncertainty	Full scale
Temperature (PT-100 type thermo-resistance)	±0.01 K	−5 to 60 °C
Temperature (T type thermocouples)	±0.5 K	−50 to 100 °C
Mass flow rate meter (Coriolis meter)	±0.2%	0–2 $kg\,s^{-1}$
Pressure transducer	20 mbar	0–25 bar
Air humidity	±0.2%	0–100%
Air temperature (PT-100 type thermo-resistance)	±0.01 K	−5 to 60 °C
Power meter (Quantum P-200)	±0.01%	100 kW

Table 2
Coil geometric parameters

Geometric parameters	Coil-1		Coil-2
Outer tube diameter, mm		9.52	
Inner tube diameter, mm		8.92	
Number of rows		4	
Number of circuits	15		11
Number of tube per rows	45		40
Tube material		Copper	
Inner tube surface		Smooth	
Inside surface area, m^2	4.28		3.81
Refrigerant side volume, $m^3 \times 10^{-3}$	9.54		8.48
Refrigerant cross-sectional area, m^2	0.94		0.69
Fin type		Wavy	
Fin material		Aluminum	
Fin spacing, mm	2.5		2.1
Air surface area, m^2	66.78		77.77

2.4. Test procedure

Within conditions contained in the EN-255 [18] and EN-12055 [19] standards, the units operated with an inlet water temperature of 45 °C and outlet water temperature of 50 °C in the heating mode (with outdoor temperature of 12 °C and relative humidity around 80% in the climatic chamber) and an inlet water temperature of 12 °C and outlet water temperature of 7 °C in the cooling mode, (with outdoor temperature of 35 °C in the climatic chamber). These conditions are referred in all figures as A12W50 and A35W7, respectively. Heating and cooling capacities from the secondary loop water mass flow rate and BPHE outlet/inlet water temperature difference were calculated following:

$$Q^{\bullet} = c_p m^{\bullet}_{\mathrm{wat}} (T_{\mathrm{out}} - T_{\mathrm{in}}) \tag{1}$$

Except for the coil design, units designated on coil-1 and coil-2 are identical. The geometric parameters of the tested coils are listed in Table 2. Note that an ideal coil should possess a high heat transfer coefficient with a low pressure drop. Both operational parameters are closely related to the mass fluxes in different parts of the HEX along the condensation and evaporation processes. The refrigerant mass flux ($G^{\bullet}$) is calculated as

$$G^{\bullet} = \frac{4m^{\bullet}_{\mathrm{r}}}{\pi \mathrm{d}_{\mathrm{i}}^2 N_{\mathrm{c}}} \tag{2}$$

2.5. Description of the ART model

For the prediction of the heat pump performance, the ART[1] model was used in both modes of operation: heating and cooling. The model incorporates a number of submodels for the integral

[1] Advanced Refrigeration Technologies.

components of the heat pump: compressor, brazed plate heat exchanger, finned tube heat exchanger, expansion devices and connecting tubes. The model and submodels have been validated using an extensive collection of experimental results by Corberán et al. [15–17].

In the present work, the model was calibrated using test results and thereof used to calculate the heat transfer coefficient and pressure drop in evaporation and condensation processes through the air heat exchanger. The submodel involving the air heat exchanger was implemented taking into account the real processes of sensible cooling, cooling with dehumidification, and sensible heating of humid air. The air heat exchanger submodel enables us to undertake a parametric study of the coil varying the influential geometric parameters (tube material and diameter, number of circuits, fin material, separation between fins, fin type, exchanger width, height and depth). To model the coil, the refrigerant side and air side HTC and pressure drop made used of semi-empirical correlations found in the specialized literature. When the coil operates as an evaporator, the VDI correlation [20] is used to determine the refrigerant side heat transfer coefficient and the Shah correlation [9] is used when it switches to a condenser. In both modes, the model used to obtain the refrigerant side pressure drop for two-phase flow operation the Chisholm–Sutherland correlation [21]. The air side heat transfer coefficient and pressure drop are calculated by means of the Chi-Chuan Wang et al. [22,23] correlations for both modes of operation.

3. Discussion of results

3.1. System performance

The variations of COP in the heat pump unit using two different coil designs as a function of superheat are shown in Fig. 3. With gradual increments in superheat the COP decreases in both

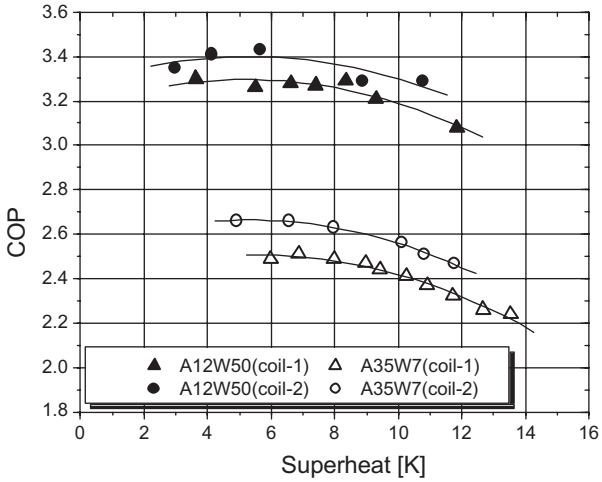

Fig. 3. COP vs. superheat using two different coil designs with R290 as working fluids. Label A35W7 (coil as condenser) refers to the cooling mode and label A12W50 (coil as evaporator) refers to the heating mode. The superheat was obtained for different positions of the expansion valve setting going from a closed to a full open position. Smaller superheat corresponds to a full open position and larger mass flow rate.

heat pump designs. The best results are rendered in the heat pump unit using coil-2 design with fewer refrigerant circuits and a higher length of circuit with a superheat of around 6 K. With respect to heat pump unit using coil-1 design the improvement is approximately 6/4% in COP, heating and cooling mode respectively. The performance elevation is linked to a higher refrigerant mass flow rate in the range of 8–13% in the cooling mode (coil as condenser) and 4–8% in the heating mode (coil as evaporator).

The variation in condensation and evaporation temperature in each operation modes are plotted in Figs. 4 and 5, respectively. In the cooling mode (coil as condenser) for a fixed evaporation temperature (Fig. 4), the condensation temperature is systematically smaller in the heat pump unit using coil-2 design. Setting a representative evaporation temperature of 0 °C, the condensation temperature decreases approximately 2 °C in the heat pump unit using coil-2 design with regard to the coil-1 design. On the other hand, in the heating mode (coil as evaporator) at the same condensation temperature (Fig. 5) the evaporation temperature is consistently higher in the heat pump unit using coil-2 design with respect to coil-1 design. Assigning a representative condensation temperature of 55 °C, for instance, the evaporation temperature increases approximately 2 °C with respect to heat pump unit using coil-1 design. This behavior of the system is obviously caused by an improved heat exchange.

The heat transfer coefficient (HTC) and the pressure drop for two different coil designs were estimated from the curve-fit of the experimental data for the calculation model mentioned above. This calculation gives a picture of what happens inside a representative circuit of the HEX taking into account the pre-selected correlations. Of course this is only realistic if the quantitative adjustment of the model to the experimental results is acceptable. In this sense, Figs. 6 and 7 show the comparison of the measured capacity and COP in both modes, heating and cooling for the two different coil designs under different test conditions with the corresponding predictions. The only free parameter used for the adjustment of the model to test results was the coil inlet air velocity distribution (which is difficult to measure accurately). Nevertheless, the air velocity found was

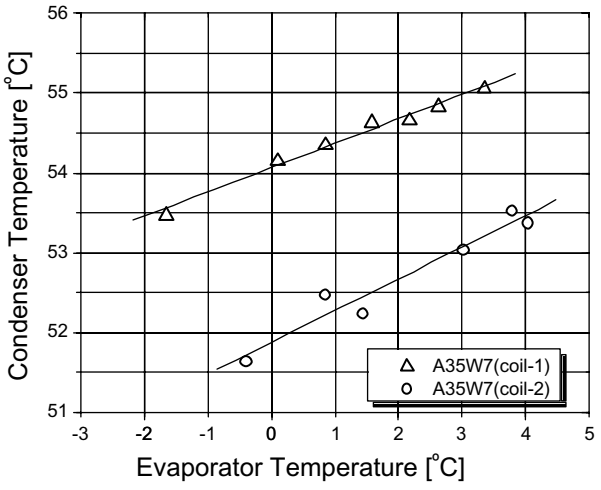

Fig. 4. Variation of refrigerant temperature with the superheat in both heat pump designs in the cooling mode. For a fixed evaporation temperature, the condensation temperature is smaller in the heat pump unit using coil-2 design.

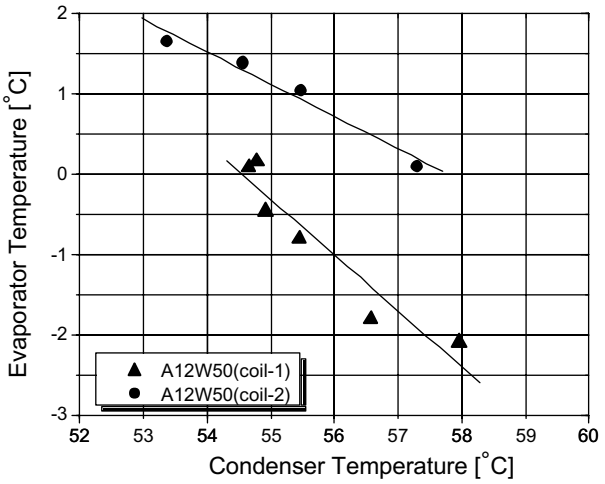

Fig. 5. Variation of refrigerant temperature with the superheat in both heat pump designs in the heating mode. For a fixed condensation temperature, the evaporation temperature is larger in the heat pump unit using coil-2 design.

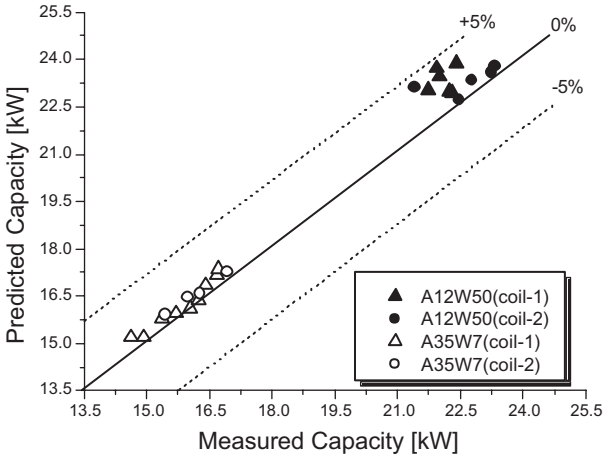

Fig. 6. Comparison of the capacity predicted by the model with the experimental results in the heat pump systems using both coil designs and modes of operation with R290 as working fluid.

very reasonable taking into account our previous estimates and the available fan data. The air velocity required for the adjustment of the experimental data in the cooling mode is $1.6\,\mathrm{m\,s^{-1}}$ and $1.5\,\mathrm{m\,s^{-1}}$ in the heating mode, respectively.

The tandem of Figs. 6 and 7 indicate that the model was able to predict capacity (Fig. 6) and COP (Fig. 7) within less 5% relative error for all tested conditions. At this point, it should be taken into consideration that for low superheat values, the model prediction could be affected by the possible presence of two-phase flow at the exit of the evaporator in the real experiment.

From the information given by the model, Figs. 8 and 9 show the distribution of HTC as a function of "relative length" along one representative refrigerant circuit at a fixed operation. In

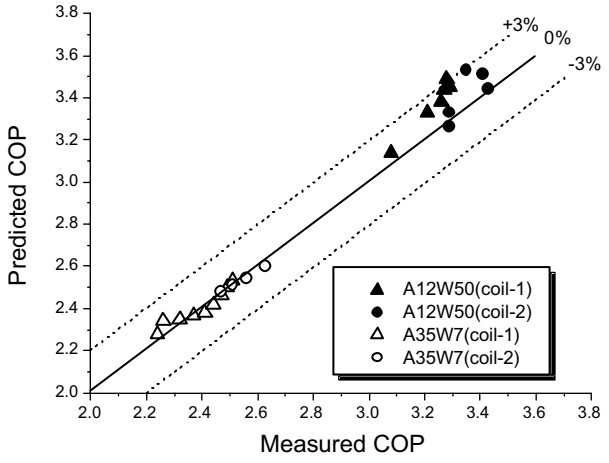

Fig. 7. Comparison of the COP predicted by the model with the experimental results.

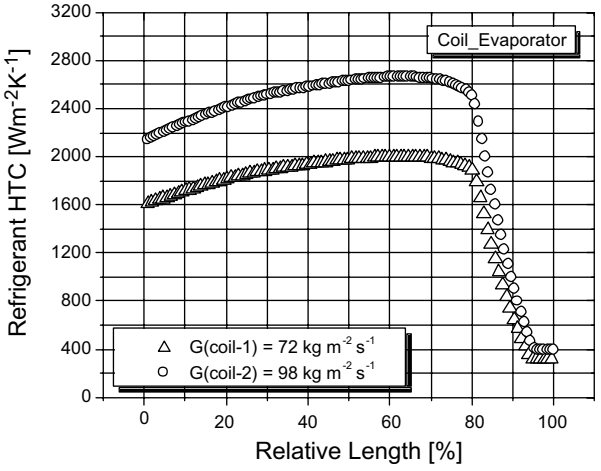

Fig. 8. Heat transfer coefficient distribution along one representative circuit in the heating mode. The term ''relative length'' refers to the position of the tube segment compared to the total length of the circuit.

the cooling mode (coil as condenser), the experimental conditions correspond to with a fixed representative subcooling of 2 K, while in the heating mode (coil as evaporator) with a fixed superheat of 6 K. As can be observed, the HTC is higher in the coil-2 design, i.e., about 33% (coil as evaporator) and 40% (coil as condenser).

On the other hand, Fig. 10 shows the calculated pressure drop as a function of mass flux. At the same operating conditions, the pressure drop is about 35% higher in the coil-2 design with regard to the coil-1 design in both modes of operation. This increase is due to the larger flow velocity, 32% increase with coil as a condenser and 26% with coil as evaporator, and the higher frictional loss due to the increased length of the refrigerant circuit in the coil-2 design.

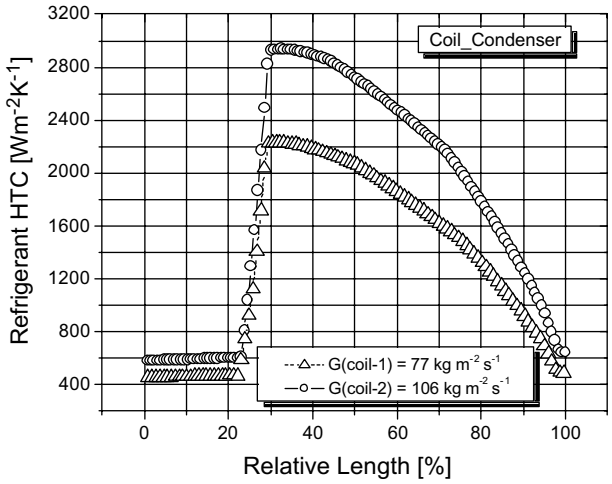

Fig. 9. Heat transfer coefficient distribution along a typical circuit in the cooling mode.

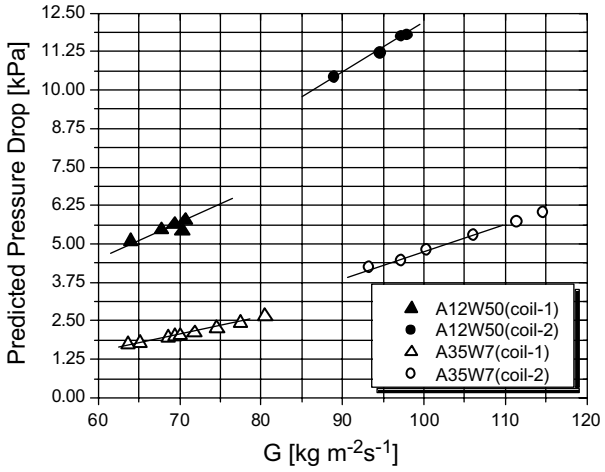

Fig. 10. Pressure drop change with the mass flux in both modes of operation and different coil designs.

4. Conclusions

In this study, the performance of an air-to-water reversible heat pump was evaluated for two coil designs at different superheat conditions using propane (R290) as the working fluid in both modes of operation: heating and cooling. The Coefficient of Performance (COP) of each coil are compared against the predictions of a simulation model. The predicted results show a good agreement with the experimental results that lie within 5% for both heat pump design and modes of operation. The experimental results indicate that the performance (COP) of the heat pump finds an optimal value at a superheat of 6–8 K depending on the heat exchanger design. An increment of the superheat leads to a deterioration of the COP.

On the other hand, it can be clearly concluded that coil-2 design yields higher local heat transfer coefficients in all calculation cells along the condensation (approximately 40%) and evaporation (approximately 33%) processes. Obviously this is tied up to a certain pressure loss penalty, about 35% in both modes of operation, which has been also estimated by the model. These results are in correspondence with the variation of the geometric parameters among both coil designs. In the coil-2 design, the length of refrigerant circuit is increased about 17% and the refrigerant cross-sectional area decreases approximately 26% with respect to coil-1 design. For the design of a given heat exchanger, an optimal relationship should exist among those parameters (number of circuits and inner tube diameter) yielding the highest possible efficiency of a given heat pump. This relationship will be investigated further using our model as a basis.

Acknowledgement

The authors acknowledge the support from the Spanish Ministry of Economy, CIATESA and AEDIE through PROFIT project no. 83 entitled "Optimización y demostración de una bomba de calor reversible con propano como refrigerante y diseminación de los resultados del proyecto".

References

[1] E. Granryd, Hydrocarbons as refrigerant—an overview, International Journal of Refrigeration 24 (2001) 15–24.
[2] Y. Hwang, A. Gado, R. Radermacher, Performance comparison of hydrocarbons R-290 with R-22 in residential heat pump system, in: Proceedings of IIR/IIF Commission B1, B2, E1 and E2, Guangzhou, China, 2002, pp. 499–506.
[3] T. Lystad, Testing of a heat pump with propane as working fluid, HPP-AN22-1, in: Proceedings Workshop Natural Working Fluids—Applications, Experience and Developments, Trondheim, Norway, October, 1995.
[4] H. Halozan, Propane for heat pumps, in: Proceedings of 19th International Congress of Refrigeration IVb, 1995, pp. 1136–1143.
[5] B. Purkayastha, P.K. Basal, An experimental study on HC290 and a commercial liquefied petroleum gas (LPG) mix as suitable replacements for HCFC22, International Journal of Refrigeration 21 (1998) 3–17.
[6] O. Pelletier, Propane as refrigerant in residential heat pumps, Engineering Licenciate Thesis Royal Institute of Technology, Stockholm, Sweden, 1998.
[7] J.M. Corberán, J. Urchueguía, J. Gonzálvez, M. Conde, T. Setaro, G. Boccardi, L. Sartori, E. Granryd, B. Palm, J. Sáez, R. Recuerda, J. Blás, E. Molinero, Development of a high efficiency heat pump using propane as refrigerant for commercial applications in Sourth Europe, in: Proceedings of the 4th IIR-Gustav Lorentzen Conference on Natural Working Fluids at Purdue University, IIF-IIR Commission B1, B2, E1, E2, 2000, pp. 141–148.
[8] X.H. Nan, A.I. Ferreira, In tube evaporation and condensation of natural refrigerant R290 (propane), in: Proceedings of the 4th IIR-Gustav Lorentzen Conference on Natural Working Fluids at Purdue University, IIF-IIR Commission B1, B2, E1, E2, 2000, pp. 239–244.
[9] M.M. Shah, A general correlation for heat transfer during film condensation inside tubes, International Journal of Heat Mass Transfer 22 (1979) 547–556.
[10] A. Cavallini, R. Zecchin, Dimensionless correlation for heat transfer in forced convection condensation, in: Proceedings of 6th International Heat Transfer Conference, Tokyo, Japan, 1974, pp. 309–313.
[11] C.K. Rice, DOE/ORNL Heat pump design model, overview and application to R22 alternatives, in: Proceedings of Third International Technical Conference "Heat Pumps in Cold Climates", August, Montreal, Canada, 1997, pp. 11–12.

[12] S.Y. Liang, T.N. Wong, G.K. Nathan, Numerical and experimental studies of refrigerant circuitry of evaporator coils, International Journal of Refrigeration 24 (2001) 823–833.
[13] G. Bigot, L. Palandre, D. Clodic, Optimized design of heat exchanger for reversible heat pump using R-407C, in: Proceedings of Eighth International Refrigeration and Air Conditioning Conference at Purdue University, 2000.
[14] J.M. Corberán, J. Gonzálvez, P. Montes, R. Blasco, ART a computer code to assist the design refrigeration and A/C equipment, in: Proceedings of Ninth International Refrigeration and Air Conditioning Conference at Purdue University, 2002.
[15] J.M. Corberán, P.F. Córdoba, S. Ortunñno, V. Ferri, P. Montes, Detailed modelling of evaporators and condensers, in: Proceedings of Eighth International Refrigeration Conference at Purdue University, 2000.
[16] J.M. Corberán, M.M. García, Modelling of plate fined tube evaporators and condensers working with R134a, International Journal of Refrigeration 21 (1998) 273–284.
[17] J.M. Corberán, J. Gonzálvez, J.F. Urchueguía, A.M. Lendoiro, Simulation of an air-to-water reversible heat pump, in: Proceedings of Eighth International Refrigeration Conference at Purdue University, 2000.
[18] EN 255, Air conditioners, liquid chilling packages and heat pumps with electrically driven compressors. Heating mode. Part 2: Testing and requirements for marking for space heating units, European Committee for Standarization, CEN TC, 1998.
[19] EN-12055, Liquid chilling packages and heat pumps with electrically driven compressors. Cooling mode. Definitions, testing and requirements, European Committee for Standardization, CEN TC, 1995.
[20] VDI Heat Atlas, in: VDI Verlag GmbH, Düsseldorf, Germany, 1990.
[21] D. Chisholm, Co. Sutherland, A theoretical basis for the Lockhart–Martinelli correlation for two-phase flow, International Journal of Heat Mass Transfer 10 (1967) 1767–1778.
[22] W. Chi-Chuan, H. Yi-Chung, L. Yur-tsai, Performance of plate tube heat exchangers under dehumidifying conditions, Journal of Heat Transfer 119 (1997) 109–117.
[23] W. Chi-Chuan, C. Yu-Juei, H. Yi-Chung, L. Yur-Tsai, Sensible heat and friction characteristics of plate fin-and-tube heat exchangers having plate fin, International Journal of Refrigeration 19 (1996) 223–230.